Surface circulation and fronts of the South Pacific Ocean, east of 120°W

Alexis Chaigneau

Centro de Investigación Oceanográfica en el Pacífico Sur-Oriental (COPAS) and Programa Regional de Oceanografía Física y Clima (PROFC), Universidad de Concepción, Concepción, Chile

Oscar Pizarro

Departamento de Geofísica, Centro de Investigación Oceanográfica en el Pacífico Sur-Oriental (COPAS), and Programa Regional de Oceanografía Física y Clima (PROFC), Universidad de Concepción, Concepción, Chile

Received 19 November 2004; revised 3 March 2005; accepted 24 March 2005; published 21 April 2005.

[1] The South Pacific surface circulation east of 120°W is studied, using satellite tracked drifters from 1979–2004. The major currents of this region are described such as the Antarctic Circumpolar, the South Pacific, the Chile-Peru and the Cape Horn Currents. We suggest the presence of a branch, exiting from the ACC between 100–120°W, and transporting subantarctic surface water toward lower latitudes. We also show the existence of an anticyclonic recirculation cell north of 35°S. Finally, based on hydrographic sections, we show that in the eastern South Pacific the core of the Subtropical front corresponds to the 14°C isotherm at 150 m depths and to the 2.7 m of dynamic height relative to 3000 m. The Subantarctic front is located by maximum temperature gradients in the range 3–8°C at 100–400 m depth. **Citation:** Chaigneau, A., and O. Pizarro (2005), Surface circulation and fronts of the South Pacific Ocean, east of 120°W, *Geophys. Res. Lett.*, *32*, L08605, doi:10.1029/2004GL022070.

1. Introduction

[2] Hydrographic measurements are sparse in the eastern South Pacific (ESP) and the badly known circulation of this region is usually depicted schematically [e.g., *Tomczak and Godfrey*, 1994]. Its main feature is the anticyclonic Subtropical Gyre, which encompasses the westward South Equatorial Current (SEC) north of 25°S, the eastward South Pacific Current (SPC) between 30–40°S, and the Chile-Peru Current (CPC) flowing equatorward along the coast [*Chaigneau and Pizarro*, 2005]. The SPC is an extension of the East Australian Current and is related to the Subtropical Convergence or Subtropical Front (STF). The STF separates relatively warm and salty subtropical water from colder and fresher subantarctic water, and carries less than 3 Sv in the ESP [*Stramma et al.*, 1995]. South of the STF, the Antarctic Circumpolar Current (ACC), driven by the strong westerly winds, transfers seawater properties between the Pacific and Atlantic oceans. It is composed of additional fronts transporting the majority of the volume water, and separating regions of particular properties. In contrast to the STF which is not continuous through Drake Passage [*Orsi et al.*, 1995], the northernmost ACC Subantarctic Front (SAF) extends all around the circumpolar belt. It is the main core of the ACC, and transports 100–150 Sv from the Pacific to the Atlantic [*Whithworth and Peterson*, 1985]. Understanding the structure and location of the fronts is important, because they are associated with strong narrow jets, they separate zones of distinct biological communities, and they can be areas of high productivity.

[3] In the last decades, the South Pacific circulation and fronts were studied based on few hydrographic sections [*Orsi et al.*, 1995; *Stramma et al.*, 1995], but there is still a lack of detail on the flow characteristics in the ESP. Using 20 years of drifter data, *Niiler* [2001] described the world ocean surface circulation on a 2° × 6° latitude-longitude grid. Here, we use 25 years of drifter data and a finer resolution, to provide an updated description of the ESP surface circulation east of 120°W, and adequate proxies for the STF and SAF identification.

2. Data and Methods

[4] The surface satellite tracked drifters data set spans the period 1979–2004 and is part of the Global Drifter Program/Surface Velocity Program (see http://www.aoml.noaa.gov). A total of 234 drogue drifters crossed the study region extending from 70–120°W and 25–60°S (Figure 1a). The Atlantic Oceanographic and Meteorological Laboratory of Miami controlled and interpolated the drifter positions to uniform 6 h intervals [*Hansen and Poulain*, 1996]. Velocity components were calculated by a centred difference scheme. To remove high-frequency energies, the data were daily averaged which results on around 120000 positions and velocities. The number of daily data on 2° × 2° bins increases from less than 50 south of 57°S to more than 200 north of 36°S (Figure 1a). The measurements are sparse along the coast, and maximum amount of data (>2000) is centred at 100°W and 30°S. To provide mean surface circulation, the velocities were averaged in each 2° × 2° grid containing more than 5 daily data. Since 98.8% of the grid boxes have more than 10 daily data, and 84% more than 40, we suppose our statistics are robust. Velocity variance ellipses and eddy kinetic energy (EKE) are computed following the methodology given by *Morrow et al.* [1994].

[5] The STF and SAF are located using both the World Ocean Atlas 2001 monthly climatology (WOA, available at http://www.nodc.noaa.gov/OC5/WOA01) and the WOCE-P18 and P19 hydrographic sections. The climatology has a horizontal resolution of 0.25°, and extends from the surface down to 1750 m depth [*Conkright et al.*, 2002]. The P18

0094-8276/05/2004GL022070

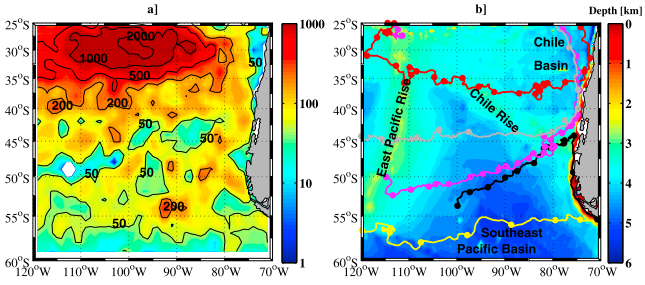

Figure 1. (a) Number of daily data over 2° × 2° area, on a logarithmic scale. (b) Examples of surface buoy trajectories over the bathymetry; each 30 day positions are indicated by a circle.

(P19, respectively) Conductivity-Temperature-Depth section was occupied in February–April 1994 (1993) along the longitude of 103°W (88°W), with station spacing less than 50 km. Frontal positions are generally defined by their subsurface temperature structure, and it exists a variety of definitions mainly adapted to the Atlantic and Indian oceans. In the ESP, frontal positions are poorly defined but the STF generally coincides with a sea surface salinity (SSS) in the range of 34.3–34.8 [*Stramma et al.*, 1995].

3. Results and Discussion

3.1. Surface Circulation

[6] As a first glance of the mean surface circulation in the study region, Figure 1b shows few selected drifter trajectories. The "yellow trajectory" flows eastward into the ACC through the Southeast Pacific Basin, and crosses the study region in about 9 months. The black and magenta pathways seem to come from the ACC and flow northeastward toward the continent. As they reach the coastal region at ~44°S, the "black drifter" moves southward into the coastal Cape Horn Current (CHC) and returns to the ACC two months later, while the "magenta drifter" is advected northward into the Chile Basin by the CPC. This drifter is then deflected westward within the SEC, exits the study area and returns into the region at ~25°S and 115°W two years later. The grey float crosses the East Pacific and Chile Rises in 8 months at the quasi constant latitude of 43–44°S before also being deflected northward by the CPC. Finally, the red trajectory, seen as the continuation of the magenta drifter, exhibits an anticyclonic circulation, with a southward moving between 110–120°W, turning eastward around 36°S and northward near the coast; the northern edge of this cell corresponds to the SEC.

[7] Figure 2c shows the mean surface circulation estimated from the drifters. *Niiler* [2001] has shown a similar figure over the world ocean using broader cell grids. Here we provide a detailed description of the ESP currents, in terms of velocity, direction and strength. West of 90°W and south of 30°S, surface currents are mainly oriented eastward and show important meridional variations: south of 50°S, the ACC surface velocities associated with the SAF are of order of 25 cm s^{-1}, and progressively decrease to 5 cm s^{-1} between 30–35°S. A secondary maximum associated with the STF of the SPC is observed at ~35°S with value of 7 cm s^{-1}. Between 40–55°S and west of 110°W, the ACC turns northeastward at it crosses the East Pacific Rise, and southeastward downstream, as was observed over other important bathymetric features [e.g., *Chaigneau et al.*, 2004].

[8] Figure 2c also shows a branch of northeastward current exporting subantarctic surface water (SSW) from the ACC (~53°S–100°W) to lower coastal latitudes (~40°S–75°W), consistently with the black and magenta trajectories shown in Figure 1b. A part of this SSW returns to the ACC through the strong coastal CHC observed south of 45°S, extending only 100–150 km offshore with typical velocities of 15–35 cm s^{-1}. During its poleward advection, SSW can mix with low salinity regional water formed by the high precipitations and river runoff along the coastal region [*Dávila et al.*, 2002]. Thus, the narrow CHC transfers low salinity and modified ACC waters into Atlantic Ocean through Drake Passage. In contrast, another part of the SSW reaching the coast is trapped into the CPC,

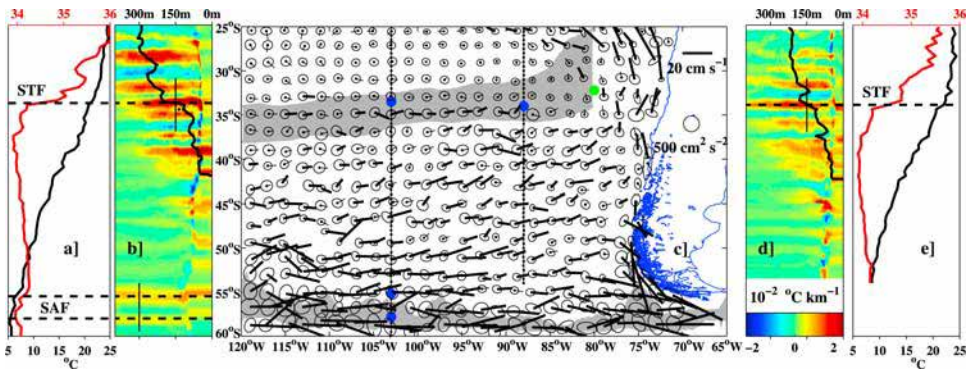

Figure 2. (a) SSS (red) and SST (black) along the 103°W WOCE-P18 section; dashed lines correspond to the STF and the two SAF branch position. (b) meridional θ gradient between 0–400 m depth along the P18 section (colour scale is given in Figure 2d); dashed lines show the front positions; thin black lines correspond to the 150 m and 300 m levels; thick black line corresponds to the 14°C isotherms. (c) Surface velocities and velocity variance ellipses from drifter measurements; velocities higher than 6 cm s^{-1} are in bold; shaded areas indicate the STF (SSS in the range 34.3–34.8) and SAF positions (maximum θ gradient in the range 3–8°C at 100–400 m depth) identified from the WOA; observed STF and SAF positions are marked (blue dots) along both the WOCE-P18 and P19 sections (dotted lines); green dot corresponds to the STF identified from the study of *Schneider et al.* [2003]; (d) and (e): as (b) and (a) but along the 88°W WOCE-P19 section.

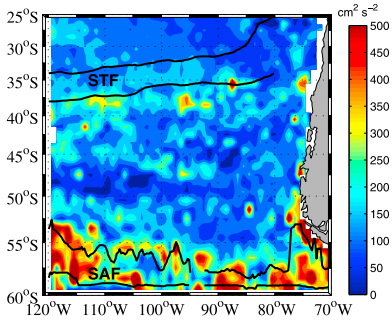

Figure 3. EKE obtained from drifter data. The mean SAF and STF positions (black contours) were identified from the WOA as in Figure 2.

transferring relatively cold and fresh water toward subtropical latitudes. This broad northwestward current, lies north of 40°S between the coast and 85°W some 1500 km offshore, and shows local surface velocity values of 15–20 cm s^{-1}.

[9] Finally, Figure 2c shows an anticyclonic recirculation cell north of 35°S, as was suggested by drifter trajectories (Figure 1b): its southern, eastern and northern edges are associated respectively with the SPC, the CPC and the SEC; between 104°W and 120°W, the southern limit of the SEC is deflected southward and returns into the SPC. This weak poleward flow of ~3 cm s^{-1}, associated with the reversal in slope of shallow isopycnals, was also observed between the dateline and 110°W from hydrographic observations at 32°S [*Wijffels et al.*, 2001].

[10] In this study, we have pointed out new current features of the ESP surface circulation. For example, the schematic of *Tomczak and Godfrey* [1994] does not include the CHC or the anticyclonic recirculation cell west of 110°W, and *Niiler*'s [2001] study, does not show the intensification of the currents associated with the fronts.

[11] Circulation derived from surface drifter measurements is a combination of geostrophic flow and wind driven Ekman currents. Ekman velocity was computed from the difference between the observed total velocity and the geostrophic flow calculated from the WOA (2001) relatively to 1750 m [*Niiler*, 2001]. The inferred Ekman drift (not shown) is oriented, in average over the region, 21° to the left of the mean satellite ERS winds. The standard deviation around this mean increases from ~20° in the region of strong westerlies, to 70° north of 40°S where the currents are weak and the winds exhibit important seasonal variability.

[12] Velocity variance ellipses (Figure 2c) reveal the anisotropic nature of the flow with an elongation principally observed in the direction of the mean currents. This anisotropy was previously observed north of 35°S in the SEC, SPC and CPC regions from drifter measurements [*Chaigneau and Pizarro*, 2005], and in the ACC from satellite altimetry [*Morrow et al.*, 1994]. Near the coast, elongated ellipses are mainly oriented parallel to the coast.

[13] Figure 3 shows the distribution of the EKE determined from drifter data. It varies from ~50 cm^2 s^{-2} in the Southeast Pacific and Chile Basins, to 300–500 cm^2 s^{-2} in the ACC. These values are higher than the 189 cm^2 s^{-2} determined from satellite altimetry data [*Qiu and Chen*, 2004], maybe due to ageostrophic motions that are not considered in the satellite measurements. EKE is also enhanced near the coast, due to several mechanisms such as the interaction of the CPC and CHC with the coastline, or the coastal upwelling front [*Blanco et al.*, 2001]. Averaged west of 90°W, the EKE decreases from 300 cm^2 s^{-2} south of 55°S to less than 100 cm^2 s^{-2} north of 26°S. Again, a secondary maximum of 250 cm^2 s^{-2} is observed at the southern edge of the STF around 37–38°S, probably associated with the generation of baroclinic instabilities.

3.2. Subtropical Front

[14] The STF is characterized by local surface velocity and EKE maxima, but both the 103°W and 88°W SSS distributions also show a northward increase from around 34 to 35 across the front (Figures 2a and 2e). These SSS values are in the range of those observed by *Stramma et al.* [1995] from other hydrographic data. The STF is also associated with important meridional temperature (θ) gradients over the 0–400 m (Figures 2b and 2d), whereas salinity (*S*) gradients are limited to the first 200 m (not shown). Sections of θ and *S* with potential density (σ_θ) as ordinate, show that the STF is also associated with strong along-isopycnal property gradients for $\sigma_\theta < 26$ kg m^{-3} (not shown).

[15] The STF shows identical characteristics at 88°W and 103°W, with an axial SSS of 34.5, an axial θ of ~14°C at 150 m depth, and similar gradients averaged over the first 150 m (Table 1). The STF can be then located from meridional SSS variations, but its main core is clearly identifiable from θ and *S* measurements at 150 m depth. In the Atlantic and Indian sectors of the Southern Ocean, the STF corresponds to the 11–12°C isotherms at 150 m depth [e.g., *Nagata et al.*, 1988]. In the ESP, the axial θ of the STF is 14°C at 150 m depth, 2–3°C higher than in other ocean basins. The difference could be attributed to the STF position, located 5–10° further north than in the Atlantic and Indian oceans.

[16] At the STF core, both the hydrographic sections also show similar dynamic height relative to 3000 m, with a value of ~2.7 m (Table 1). This suggests that using maps of sea surface height, obtained from altimetry measurements and dynamic topography, it may be possible to study the spatio-temporal STF variability corresponding to the 2.7 m dynamic height contour. Based on a similar method, *Sokolov and Rintoul* [2002] have determined the paths and variability of the ACC fronts south of Tasmania.

Table 1. Characteristics of the STF From the February–April 1993 (1994, Respectively) 88°W (103°W) P19 (P18) Section[a]

	SSS	SST (°C)	S_{150m}	θ_{150m} (°C)	$\overline{\nabla S}^{0\rightarrow150m}$ (km^{-1})	$\overline{\nabla\theta}^{0\rightarrow150m}$ (°C km^{-1})	DH (m)
P19	34.5	22.0	34.3	13.9	0.004	0.016	2.68
88°W-34.5°S	34.2 → 34.8						
P18	34.5	21.1	34.4	13.9	0.005	0.019	2.70
103°W-33.8°S	34.2 → 34.9						

[a]Abbreviations used: SSS and SST: sea surface salinity (and the range) and temperature; S_{150m} and θ_{150m}: salinity and temperature at 150 m depth; $\overline{\nabla S}^{0\rightarrow150m}$ and $\overline{\nabla\theta}^{0\rightarrow150m}$: meridional salinity and temperature gradients averaged over 0–150 m depth; DH: dynamic height relative to 3000 m depth.

[17] Due to the limited number of hydrographic data in the study region, the WOA does not reproduce conveniently the STF position in terms of θ and *S* gradients. The objective analyses and the optimum interpolation schemes applied to the sparse in-situ data [*Conkright et al.*, 2002], may also be responsible for the shift of the 14°C isotherm at 150 m depth, which is found, east of 90°W, 4–5° further north than the observed STF positions. Nevertheless, Figure 2c shows that the 34.3 and 34.8 SSS contours, corresponding to the typical values across the STF, include the two STF positions identified from the WOCE sections, and also a more eastern frontal position (80°W, 32.2°S) determined from the study of *Schneider et al.* [2003].

3.3. Subantarctic Front

[18] The SAF has also a clear signature on the surface velocity and EKE fields with typical values of 20 cm s^{-1} and 300 cm^2 s^{-2}. During its circumpolar pathway, the SAF can exhibit multiple filaments, and along the 103°W section, two branches centred at 58°S and 55.5°S, are associated with strong meridional θ gradients (Figure 2b). The definition given by *Belkin* [1990] in the Atlantic Ocean is also valid in the ESP. The SAF is associated with maximum θ gradient in the range 3–8°C at 100–400 m depth. Using this criterion, the WOA reproduces conveniently the SAF positions (Figures 2b and 3). At 300 m depth, the southern and northern SAF branches show axial θ of 4°C and 5°C respectively, and axial *S* of 34.1–34.2 (not shown). Nevertheless, based only on the 103°W WOCE-P18 data, we can not determine more appropriate criteria than the proxy of *Belkin* [1990] for the location of the SAF.

[19] Across the SAF, there is a nearly density compensation in the mixed layer associated with weak meridional SSS and SST variations (Figure 2a). Below the mixed layer, θ decreases and *S* increases to the south, contributing to a southward increase in σ_θ (not shown) which is part of the dynamical balance related to the strong eastward velocities transporting more than 135 Sv [*Whithworth and Peterson*, 1985]. Each of the two SAF branches coincides with enhanced along-isopycnal gradients of θ and *S* for $\sigma_\theta <$ 27.3 kg m^{-3}. Finally, in the upper 100 m, θ gradients associated with the SAF are found 0.5–1° further north than their deeper counterparts (Figure 2b), maybe due to a northward Ekman transport of the shallow layer by the strong westerly winds, as also observed south of Tasmania by *Chaigneau and Morrow* [2002].

4. Summary

[20] Based on 25 years of drifter data, the ESP surface circulation was studied. From south to north, we described the strong ACC associated with the SAF, the SPC where the STF is found, and north of 35°S we observed the presence of an anticyclonic recirculation cell. We have also shown the existence of a branch exiting from the ACC and transporting SSW toward coastal regions at lower latitudes. Near the coast the southward CHC and the northwestward CPC were also characterized.

[21] In agreement with previous studies [*Stramma et al.*, 1995; *Chaigneau and Morrow*, 2002], we have shown in the ESP, that the STF is more easily identifiable from SSS variations than from SST gradients. It also corresponds to the 14°C isotherms at 150 m depth, and to the 2.7 m of dynamic height relative to 3000 m. The SAF branches are associated with strong θ gradients in the range 3–8°C at 100–400 m depth. These criteria provide robust proxies for future studies of fronts location and variability in the ESP.

[22] **Acknowledgments.** Drifter data were provided by the National Oceanic and Atmospheric Administration (NOAA). A.C. was supported by ECOS-SUD and Fundación Andes grant D-13615. This work was also supported by the Chilean National Research Council (FONDAP-COPAS). We thank the two anonymous reviewers for their helpful comments.

References

Belkin, I. M. (1990), Hydrological fronts of the Indian subantarctic, in *The Antarctic: The Committee Reports*, vol. 29, edited by M. E. Vinogradow and M. V. Flint, pp. 119–128, Nauka, Moscow.

Blanco, J. L., A. C. Thomas, M.-E. Carr, and P. T. Strub (2001), Seasonal climatology of hydrographic conditions in the upwelling region off northern Chile, *J. Geophys. Res.*, *106*, 11,451–11,467.

Chaigneau, A., and R. M. Morrow (2002), Surface salinity and temperature variations between Tasmania and Antarctica, 1993–1999, *J. Geophys. Res.*, *107*(C12), 8021, doi:10.1029/2001JC000808.

Chaigneau, A., and O. Pizarro (2005), Mean surface circulation and mesoscale turbulent flow characteristics in the eastern South Pacific, from satellite tracked drifters, *J. Geophys. Res*, doi:10.1029/2004JC002628, in press.

Chaigneau, A., R. Morrow, and S. Rintoul (2004), Seasonal and interannual variations of the mixed layer in the Antarctic zone south of Tasmania, *Deep Sea Res., Part I*, *51*, 2047–2072.

Conkright, M. E., R. A. Locarnini, H. E. Garcia, T. D. O'Brien, T. P. Boyer, C. Stephens, and J. I. Antonov (2002), *World Ocean Atlas 2001: Objective Analyses, Data Statistics, and Figures* [CD-ROM], NOAA, Silver Spring, Md.

Dávila, P. M., D. Figueroa, and E. Müller (2002), Freshwater input into the coastal ocean and its relation with salinity distribution off austral Chile (35–55°S), *Cont. Shelf Res.*, *22*, 521–534.

Hansen, D. V., and P.-M. Poulain (1996), Quality control and interpolations of WOCE-TOGA drifter data, *J. Atmos. Oceanic Technol.*, *13*, 900–909.

Morrow, R., R. Coleman, J. Church, and D. Chelton (1994), Surface eddy momentum flux and velocity variances in the Southern Ocean from Geosat altimetry, *J. Phys. Oceanogr.*, *24*, 2050–2071.

Nagata, Y., Y. Michida, and Y. Umimura (1988), Variations of positions and structures of the ocean fronts in the Indian Ocean sector of the Southern Ocean in the period from 1965 to 1987, in *Antarctic Ocean and Resources Variability*, edited by D. Salirhage, pp. 92–98, Springer, New York.

Niiler, P. (2001), The world ocean surface circulation, in *Ocean Circulation and Climate: Observing and Modelling the Global Ocean*, *Int. Geophys. Ser.*, vol. 77, edited by G. Siedler, J. Church, and J. Gould, pp. 193–204, Elsevier, New York.

Orsi, A. H., T. Whithworth, and W. D. Nowlin (1995), On the meridional extent and fronts of the Antarctic Circumpolar Current, *Deep Sea Res., Part I*, *42*, 641–673.

Qiu, B., and S. Chen (2004), Seasonal modulations in the eddy field of the South Pacific Ocean, *J. Phys. Oceanogr.*, *34*, 1515–1527.

Schneider, W., R. Fuenzalida, E. Rodríguez-Rubio, J. Garcés-Vargas, and L. Bravo (2003), Characteristics and formation of eastern South Pacific Intermediate Water, *Geophys. Res. Lett.*, *30*(11), 1581, doi:10.1029/2003GL017086.

Sokolov, S., and S. R. Rintoul (2002), Structure of Southern Ocean fronts at 140°E, *J. Mar. Syst.*, *37*, 151–184.

Stramma, L., R. G. Peterson, and M. Tomczak (1995), The South Pacific Current, *J. Phys. Oceanogr.*, *25*, 77–91.

Tomczak, M., and J. S. Godfrey (1994), *Regional Oceanography: An Introduction*, 442 pp., Elsevier, New York.

Whithworth, T., III, and R. G. Peterson (1985), Volume transport of the Antarctic Circumpolar Current from bottom pressure measurements, *J. Phys. Oceanogr.*, *15*, 810–816.

Wijffels, S. E., J. M. Toole, and R. Davis (2001), Revisiting the South Pacific subtropical circulation: A synthesis of World Ocean Circulation Experiment observations along 32°S, *J. Geophys. Res.*, *106*, 19,481–19,513.

A. Chaigneau and O. Pizarro, COPAS/PROFC, Universidad de Concepción, Barrio Universitario Concepción, Concepción, Chile. (chaigneau@profc.udec.cl)